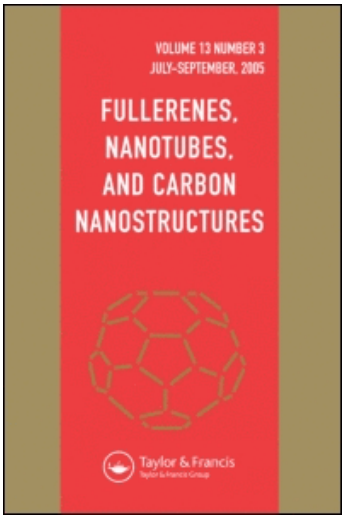

Fullerenes, Nanotubes and Carbon Nanostructures
Publication details, including instructions for authors and subscription information:
http://www.informaworld.com/smpp/title~content=t713597253

Nanoresonator Based on Relative Vibrations of the Walls of Carbon Nanotubes

E. Bichoutskaia[a]; A. M. Popov[b]; Y. E. Lozovik[bc]; O. V. Ershova[c]; I. V. Lebedeva[cde]; A. A. Knizhnik[de]
[a] Department of Chemistry, University of Nottingham, Nottingham, United Kingdom [b] Institute of Spectroscopy, Russian Academy of Sciences, Troitsk, Moscow Region, Russia [c] Moscow Institute of Physics and Technology, Dolgoprudny, Moscow Region, Russia [d] RRC "Kurchatov Institute,", Moscow, Russia [e] Kintech Lab Ltd, Moscow, Russia

Online publication date: 27 October 2010

To cite this Article Bichoutskaia, E. , Popov, A. M. , Lozovik, Y. E. , Ershova, O. V. , Lebedeva, I. V. and Knizhnik, A. A.(2010) 'Nanoresonator Based on Relative Vibrations of the Walls of Carbon Nanotubes', Fullerenes, Nanotubes and Carbon Nanostructures, 18: 4, 523 — 530
To link to this Article: DOI: 10.1080/1536383X.2010.488524
URL: http://dx.doi.org/10.1080/1536383X.2010.488524

Fullerenes, Nanotubes, and Carbon Nanostructures, 18: 523–530, 2010

ISSN: 1536-383X print / 1536-4046 online
DOI: 10.1080/1536383X.2010.488524

Taylor & Francis
Taylor & Francis Group

Nanoresonator Based on Relative Vibrations of the Walls of Carbon Nanotubes

E. BICHOUTSKAIA[1], A. M. POPOV[2], Y. E. LOZOVIK[2,3], O. V. ERSHOVA[3], I. V. LEBEDEVA[3,4,5] AND A. A. KNIZHNIK[4,5]

[1]Department of Chemistry, University of Nottingham, Nottingham, United Kingdom
[2]Institute of Spectroscopy, Russian Academy of Sciences, Troitsk, Moscow Region, Russia
[3]Moscow Institute of Physics and Technology, Dolgoprudny, Moscow Region, Russia
[4]RRC "Kurchatov Institute," Moscow, Russia
[5]Kintech Lab Ltd, Moscow, Russia

A new type of ultrahigh frequency resonator based on the relative vibrations of carbon nanotubes walls is proposed. Microcanonical molecular dynamics simulations performed for a model resonator based on the (9,0)@(18,0) double-walled carbon nanotube with the movable outer wall give the value of frequency equal to 130 GHz and the quality factor up to 500. Possible applications of the resonator are discussed. The estimated mass sensitivity of the mass sensor based on the proposed resonator reaches the atomic mass limit at liquid helium temperature. The possibility of resonator based on relative vibrations of graphene layers is also considered.

Keywords Carbon nanotube, Graphene, Mass sensor, Resonator

Introduction

Nanoelectromechanical systems (NEMS) might radically change fundamental measurements at the molecular scale. Mechanical nanoresonators with the mass in the range of hundreds of femtograms and the operational frequencies in the region of 100 MHz to 1 GHz can now be fabricated (see, e.g., 1–4). Due to small effective mass of their vibrating parts and small moment of inertia, nanoresonators can serve as sensitive mass sensors capable of less than 10^{-21} g resolution (4). Two types of mechanical motion used up to now in nanomechanical resonators are flexural and torsional vibrations.

Due to the unique electric and mechanical properties, carbon nanotubes are considered as a promising material for use in NEMS. Significant progress has been made in constructing resonators based on the transverse vibrations of carbon nanotubes (3,4). In this paper, a new type of mechanical motion is considered for the use in ultrahigh frequency resonators, the relative vibrations of the components. Namely, we propose a resonator based on relative vibrations of carbon nanotube walls. The possible application of this resonator as a mass sensor is considered. A major advantage of such a resonator over the existing systems, as

Address correspondence to A. M. Popov, Institute of Spectroscopy, Russian Academy of Sciences, 142190, Troitsk, Moscow Region, Russia. E-mail: am-popov@isan.troitsk.ru

described in (1–4), is that its resonant frequency does not depend on the size of the resonator or on the position of an adsorbed particle which mass is measured.

The paper is organized as follows. Section 2 presents calculations of the frequencies of the relative axial and rotational vibrations for different double-walled nanotubes (DWNTs). Section 3 is devoted to microcanonical molecular dynamics (MD) simulations of a model resonator based on the (9,0)@(18,0) DWNT and resonator based on the relative vibrations of graphene layers. Section 4 contains estimates of the mass sensitivity of the new nanotube-based resonators used as the mass sensors. Our conclusions are summarized in section 5.

Interaction and Vibrational Frequencies of the Walls of Carbon Nanotubes

With the exception of the calculations (5) of the frequency of the rotational vibration in a (5,5)@(10,10) DWNT, the relative vibrations of the walls have not been previously studied. For DWNTs with the interwall distance in the range of 3.4 to 3.7 Å the calculations show that the radial displacements of the walls from coaxial position lead to significant increase in the interwall interaction energy (5,6). Therefore, the relative axial and rotational vibrations of the walls do not follow by the radial displacements. In this case the frequencies of these vibrations can be calculated using the dependence of the interwall interaction energy, U, only as a function of the angle of the relative rotation of the walls, φ, and their relative displacement, z. According to semi-empirical (7,8), and *ab initio* calculations (9) for the nonchiral commensurate (n_1,n_1)@(n_2,n_2) armchair and the $(n_1,0)$@$(n_2,0)$ zigzag DWNTs the interwall interaction energy can be interpolated using the first two harmonics of the Fourier expansion:

$$U(\phi,z) = U_0 - U(\phi) - U(z) = U_0 - \frac{\Delta U_\phi}{2}\cos\left(\frac{2\pi}{\delta_\phi}\phi\right) - \frac{\Delta U_z}{2}\cos\left(\frac{2\pi}{\delta_z}z\right), \qquad (1)$$

where U_0 is the average interwall interaction energy, ΔU_ϕ and ΔU_z are the energy barriers to the relative rotation and sliding of the walls. For the considered case of commensurate walls U_0, ΔU_ϕ and ΔU_z are proportional to the length of the overlap between the walls. Periods of the rotation and sliding between the equivalent positions are defined as $\delta_\phi = \pi N/(n_1 n_2)$ and $\delta_z = l_c/2$, where N is the greatest common factor of integers n_1 and n_2, and l_c is the length of the unit cell of DWNT. For DWNTs with compatible rotational symmetry of the walls ($N = n_1$), the energy barrier to the relative rotation, ΔU_ϕ, can be significant. For DWNTs with incompatible rotational symmetry of the walls ($N = 1$), both *ab initio* [10] and semi-empirical (7) results show that the dependence of the interwall interaction energy on the angle ϕ is typically very small; thus the second term in expansion (1) can be neglected.

To calculate the frequencies of the relative vibrations of the walls, the second and third terms in expansion (1) of the interwall interaction energy surface are interpolated near the minimum using the harmonic potential as follows:

$$U(z) = \frac{1}{2}k_z z^2, \; U(\phi) = \frac{1}{2}k_\phi \phi^2 \qquad (2)$$

where

$$k_z = \frac{8n_2 l_{ov}\Delta U_z}{l_c}\left(\frac{2\pi}{l_c}\right)^2, \; k_\phi = \frac{8n_2 l_{ov}\Delta U_\phi}{l_c}\left(\frac{n_1 n_2}{N}\right)^2 \qquad (3)$$

Here l_{ov} is the length of the overlap between the walls. Here and below ΔU_z and ΔU_ϕ are the barriers per atom of the outer wall.

The frequencies v_z and v_ϕ of the axial and rotational vibrations of the walls can be determined as:

$$v_z = \frac{1}{2\pi}\sqrt{\frac{k_z}{M}},\ v_\phi = \frac{1}{2\pi}\sqrt{\frac{k_\phi}{J}} \tag{4}$$

Here the mass M and the moment of inertia J correspond to the moving wall. If the DWNT is not fixed between the electrodes and is floating without friction, the reduced mass and the reduced moment of inertia of both moving walls should be used.

The frequencies of the axial and rotational vibrations do not depend on the length of DWNT if both walls have the same length or if the longer wall is fixed and not moving. In such cases, the length of the overlap l_{ov} between the walls is equal to the length of vibrating wall(s). Inserting expressions (3) for k_z and k_ϕ, into equation (4) together with the relevant expressions for M and J, the frequencies of the relative axial vibrations of the walls can be defined as follows:

$$v_{z,1} = \frac{1}{l_c}\sqrt{\frac{2n_2\Delta U_z}{n_1 m_C}},\ v_{z,2} = \frac{1}{l_c}\sqrt{\frac{2\Delta U_z}{m_C}},\ v_{z,12} = \frac{1}{l_c}\sqrt{\frac{2(n_1+n_2)\Delta U_z}{n_1 m_C}}, \tag{5}$$

where $v_{z,1}$ and $v_{z,2}$ are the frequencies of the axial sliding vibrations of the inner and outer wall, correspondingly, $v_{z,12}$ is the frequency of the relative axial sliding vibrations of the walls, and m_C is the mass of a carbon atom. Similarly, the frequencies $v_{\phi,1}$, $v_{\phi,2}$ and $v_{\phi,12}$ of the rotational vibrations of the walls are given by the following expressions:

$$\begin{aligned} v_{\phi,1} &= \frac{n_2}{\pi N R_1}\sqrt{\frac{n_1 n_2 \Delta U_\phi}{2m_C}},\ v_{\phi,2} = \frac{n_1 n_2}{\pi N R_2}\sqrt{\frac{\Delta U_\phi}{2m_C}}, \\ v_{\phi,12} &= \frac{n_2}{\pi N R_1 R_2}\sqrt{\frac{n_1\left(n_1 R_1^2 + n_2 R_2^2\right)\Delta U_\phi}{2m_C}} \end{aligned} \tag{6}$$

where R_1 is the radius of the inner wall, and R_2 is the radius of the outer wall.

To estimate the frequencies of the relative vibrations of the walls, we have performed calculations of the interwall interaction energy surfaces $U(\phi,z)$ for different DWNTs using empirical potentials (see detailed methodology in (11,12)). Interaction between carbon atoms of the inner and the outer walls was described using the Lennard–Jones 12-6 potential $u = 4\varepsilon\left((\sigma/r)^{12} - (\sigma/r)^6\right)$ with parameters $\varepsilon = 3.73$ meV and $\sigma = 0.34$ nm taken from the AMBER database (13). The cut-off distance of the Lennard–Jones potential was taken to be 6.0–12.0 nm. The infinite inner wall was considered and periodic boundary conditions were applied along the principal axis of the DWNT. The length of the simulation cell was 6.4–13.2 nm. The outer wall was 2 nm in length. In the calculations, the outer wall was rigidly shifted and rotated with respect to the inner wall.

Our calculations confirm that the interwall interaction energy surface is described well by formula (1). The energy barriers and the corresponding frequencies of the relative vibrations of the walls are given in Table 1. The found values of the energy barriers are in good agreement with the previous semi-empirical calculations (7). These values of the energy barriers are an

Table 1
Calculated barriers ΔU_z and ΔU_ϕ (in meV/atom) for the relative sliding and rotation of the walls per atom of the outer wall and frequencies $\nu_{z,2}$ and $\nu_{\phi,2}$ (in GHz) of the corresponding vibrations for DWNTs of different outer wall radius R_2 (in nm) and interwall distance ΔR (in nm)

			Static calculations				MD Simulations
DWNT	R_2	ΔR	ΔU_z	ΔU_ϕ	$\nu_{z,2}$	$\nu_{\phi,2}$	$\nu_{z,2}$
(4,4)@(10,10)	0.68	0.41	$6.9\cdot10^{-5}$	$<2\cdot10^{-8}$	4.3	<0.09	
(5,5)@(11,11)	0.75	0.41	$7.5\cdot10^{-5}$	$<5\cdot10^{-8}$	4.5	<0.3	
(6,6)@(12,12)	0.82	0.41	$8.0\cdot10^{-5}$	$4.1\cdot10^{-4}$	4.1	6.1	
(5,5)@(10,10)	0.68	0.34	$8.1\cdot10^{-3}$	$2.3\cdot10^{-2}$	47	46	36
(6,6)@(11,11)	0.75	0.34	$8.4\cdot10^{-3}$	$<5\cdot10^{-8}$	48	<0.4	37
(9,0)@(18,0)	0.71	0.35	$1.8\cdot10^{-1}$	$9.0\cdot10^{-6}$	130	1.6	130
(10,0)@(20,0)	0.79	0.39	$2.5\cdot10^{-2}$	$3.2\cdot10^{-7}$	48	0.30	46

order of magnitude smaller than the values obtained using the density functional theory and tight-binding method (see (10,14) and references in (14)). However, there is a qualitative agreement with the results of the density functional theory calculations (10):

1. Although the values of the radii and interwall distances are very close in the armchair (5,5)@(10,10) DWNT and the zigzag (9,0)@(18,0) DWNT, the barrier to the relative sliding of the walls is an order of magnitude higher in the (9,0)@(18,0) DWNT, while the barrier to the relative rotation of the walls is significantly higher in the (5,5)@(10,10) DWNT (see Table 1). This fact is reflected in the high frequency of telescopic vibrations in the (9,0)@(18,0) DWNT and high frequency of rotational vibrations in the (5,5)@(10,10) DWNT.
2. As it is seen from Table 1, the barrier to the relative rotation of the nanotube walls decreases significantly on small increasing the interwall distance.
3. For DWNTs with incompatible rotational symmetry, the barrier for the rotation is very small.

Ultrahigh Frequency Resonator: Molecular Dynamics Simulations

We suppose that the relative vibrations of the nanotube walls considered above can be used in ultrahigh frequency resonators. The proposed ultrahigh frequency resonator consists of a DWNT with a long inner wall attached to the source and drain electrodes, and the short outer wall (shuttle) that can move along the inner wall between the source and drain electrodes and/or rotate about the nanotube axis. In principle, the resonator could be built from multi-walled carbon nanotubes, analogous to the design of recently realized nanotube-based motors (15). Whereas making of such resonator is now possible, inducing and detecting the relative vibrations of the nanotubes walls with the amplitudes of subangstroem scale at such extremely high resonant frequencies becomes a real challenge. We propose that the vibrations of the walls can be excited by applying a subterahertz radiation. The conductivity of a nonchiral commensurate DWNT with a short outer wall depends significantly on position of the outer wall in subangstroem scale (16). In this case the conductivity of this DWNT is a function of the

amplitude of the outer wall vibrations (see details in (17), where the operation of nanothermometer based on thermal vibrations of a short wall of DWNT is considered). So measurements of the dependence of the conductivity between the source and drain electrodes on the applied frequency can be used to determine the resonance frequency.

The microcanonical MD simulations have been performed to study the frequencies and Q-factors of the DWNT-based resonators with the movable outer wall. In these simulations, the covalent carbon–carbon interactions were described using the empirical Brenner potential (18). To calculate the frequencies of the resonators, the MD simulations were performed at zero initial temperature. The time step was 0.1 fs. The duration of each simulation was chosen so that to involve two to three periods of the oscillation. The configuration of the nanotube was optimized at zero temperature. At the beginning of the simulations, the outer wall was shifted along the nanotube axis at the distance of 0.1 Å and released with zero center-of-mass velocity. The inner wall was fixed at three atoms. The results of the frequency calculations for the relative axial vibrations of the walls using the MD simulations are given in Table 1. It is seen that they agree with the results of the static calculations using formula (5) within the 20% accuracy (see Table 1). To estimate the frequency of the relative rotational vibration of the walls in the (5,5)@(10,10) DWNT, the outer wall was given the initial rotational kinetic energy equal to about 1/10 of the barrier to the rotation. The frequency of the rotational vibration in the (5,5)@(10,10) DWNT was found to be 48 GHz, in good agreement with formula (6) (see Table 1).

The Q-factor of the (9,0)@(18,0) DWNT was also estimated through the MD simulations. In these calculations, small free oscillations of the outer wall along the principal axis of the DWNT were allowed with the initial amplitude of 0.58 Å. Ten simulations with different initial distributions of velocities of the atoms were performed at liquid nitrogen temperature of 77 K, and 14 simulations were performed at liquid helium temperature of 4.2 K. The durations of each simulation were about 100 ps and 130 ps and the time steps were 0.1 fs and 0.3 fs at the temperature values of 4.2 K and 77 K, respectively. In the latter case, the time step is two orders of magnitude smaller than the period of the thermal vibrations of carbon atoms.

Typical examples of the time dependences of the displacement of the outer wall along nanotube axis presented in Figure 1 show the damped oscillations of this wall. Small beats were regularly seen at temperature of 4.2 K (see Figure 1a). The average Q-factor obtained for temperature of 4.2 K is $Q=540\pm240$. At temperature of 77 K, strong beats of amplitude of oscillations were observed in three simulations (see Figure 1b), and small beats were observed in four simulations. Since the presence of beats leads to a noticeable uncertainty in Q-factor calculation, the Q-factor at temperature of 77 K was averaged over the three simulations in which there were no beats (see Figure 1c). The obtained value of the Q-factor is $Q=160\pm80$. Since the energy loss per one oscillation period and the thermal kinetic energy per degree of freedom are of the same order of magnitude, considerable thermodynamic fluctuations of the energy of the relative axial vibration of the outer wall are observed at the MD simulations. These thermodynamic fluctuations cause a large error of the Q-factor calculations. Furthermore, the Q-factor averaged over one simulation is sensitive to the initial distribution of coordinates and velocities of carbon atoms. Note that the thermodynamic fluctuations in the DWNT-based gigahertz oscillator and the restrictions imposed by the fluctuations on the minimum size of this NEMS were studied in (12) using MD simulations and theoretical analysis in the framework of the fluctuation-dissipation theorem.

The calculated values of the Q-factors of the resonator are of the same order of magnitude as the Q-factors of gigahertz oscillators based the large telescopic oscillation of inner wall of DWNT. The Q-factor values of such oscillators calculated and estimated in (12) from the data previously obtained in MD simulations are $Q=300$–800 at low temperatures of

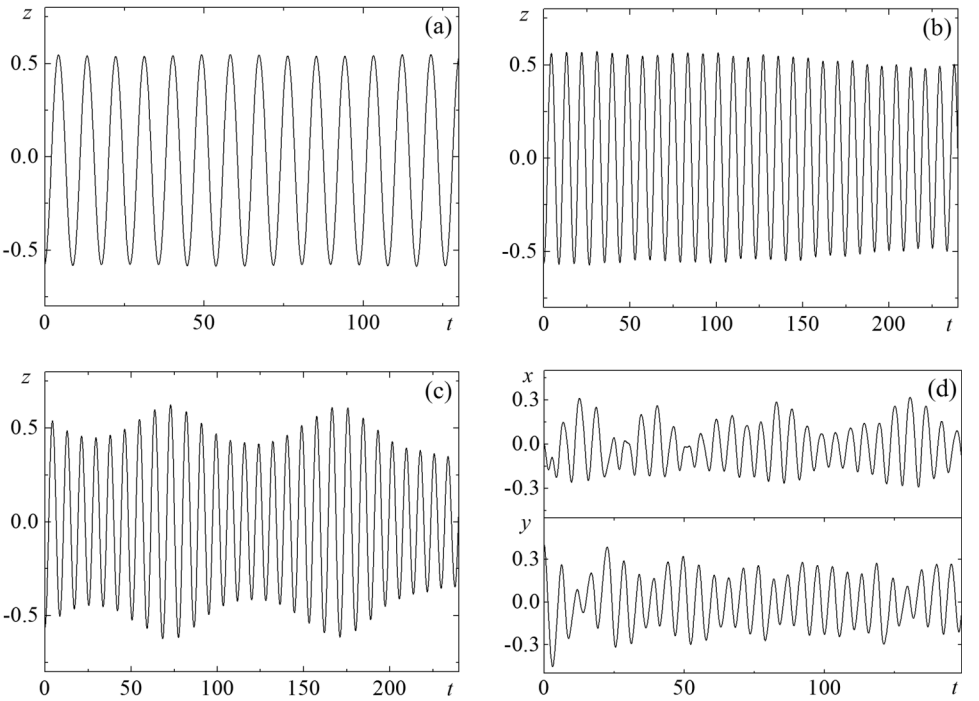

Figure 1. The displacement (in Å) of the movable element of the resonator as a function of time (in ps): (a, b, c) outer wall of the (9,0)@(18,0) DWNT along the axis at **(a)** $T = 4.2$ K and **(b, c)** $T = 77$ K; **(d)** graphene flake on graphene surface at $T = 4.2$ K (the solid line corresponds to the zigzag direction, and the dashed line corresponds to the perpendicular armchair direction).

0 to 8 K. The MD simulations performed here for the resonator show significant increase in the values of Q-factor with the decrease in temperature similarly to the increase observed for DWNT-based gigahertz oscillator (12).

The origin of the beats observed in the simulations for the (9,0)@(18,0) DWNT-based resonator can be explained by resonances between the vibrational mode under consideration and the other vibrational modes of the system. The presence of the resonances should decrease the Q-factor. Note that according to the results of our frequency calculations, there should be a resonance between the rotational and axial relative vibrations of the walls for the (5,5)@(10,10) DWNT (see Table 1). So probably the (5,5)@(10,10) DWNT-based resonator has a low Q-factor.

We also present preliminary results of MD simulations of a resonator based on the relative vibrations of graphene layers along graphene plane. The system consisting of an infinite graphene layer and 2.0 nm×2.1 nm graphene flake at temperature of 4.2 K was considered. The simulation cell was 4.2 nm×4.3 nm in size. The cut-off distance of the Lennard-Jones potential was taken to be 2.0 nm. The time step was 0.4 fs. At the beginning of the simulation, the flake was shifted from the energy minimum by 0.4 Å along the zigzag direction.

The oscillation of the flake with the frequency 0.17 THz was observed along the initial direction (see Figure 1d). However, the amplitude of this oscillation did not remain constant. The similar oscillation along the perpendicular direction was easily excited. The point is that

in harmonic approximation, these two vibrations have the same frequency. Therefore the energy exchange between these vibrations is very fast. In spite of this, the graphene system can still be regarded as a resonator but with two degrees of freedom (as opposed to the DWNT based resonator). This problem will be considered in detail elsewhere.

Possible Applications of Ultrahigh Frequency Resonator

The proposed design of the resonator exhibits promise as a precise mass sensor. Such a mass sensor operates by measuring the frequency shift of the resonance as additional mass; that is, a molecule, a molecular cluster, or a nanoparticle is adsorbed on the vibrating short outer wall of the proposed resonator. The upper estimate for the mass sensitivity related to the thermomechanical noise in a nanoresonator can be found as follows (1):

$$\delta M \leq \frac{2M}{Q}\sqrt{\frac{k_B T}{2\pi E}} \tag{7}$$

where T is the temperature and E is the energy of the vibration of movable element.

In the proposed model resonator based on the (9,0)@(18,0) DWNT, the mass of the oscillating (18,0) wall equals to $360m_C$, thus based on the Q-factor values calculated above, the mass sensitivity of the resonator can be estimated as $0.7m_C$ and $0.05m_C$ for temperatures of 77 K and 4.2 K, respectively. Sensitivity of the resonator can be improved by decreasing temperature, as well as the length and diameter of the moving outer wall. Therefore, the mass sensitivity of the proposed resonator can be less than the mass of a single carbon atom. An advantage of the new design compared to the cantilever resonators is that the relation between shifts in the resonant frequency and changes in the mass depends only on the geometry of the resonator, not on the position of adsorbed particle.

The recently fabricated Barreiro motor (15), in which a nano-object was attached to a short outer wall of a multi-walled carbon nanotube that could move along its inner core, can be used as a part of resonator for the atomic resolution mass measurements. For the experimental dimensions of the outer wall reported in (15) as 300 nm in length and 7 nm diameter, the sensitivity of the Barreiro device estimated using equation (7) would be $20m_C$ for the Q-factor of 160 and $1.4m_C$ for the Q-factor of 540.

Conclusions

The relative vibrations of the DWNT walls are proposed to be used in ultrahigh frequency resonators. The calculated frequencies of these resonators lie in the range of 1 to 130 GHz for the axial vibrations and up to 50 GHz for the rotational vibrations and do not depend on the length of the walls in the case of one long fixed wall and another short movable wall. Our MD simulations of the model resonator based on such vibrations confirm the values of the frequencies obtained by the static calculations. The MD simulations give the values of the Q-factor of the model resonator equal to Q=160 at 77 K and Q=540 at 4.2 K. Beats arising from a resonance between the relative vibrations of the walls and other modes of the system are observed in the simulations. The estimations show that the resonator considered can be used for mass sensing with the mass sensitivity less than the mass of a single carbon atom. In the proposed design, the frequency depends only on the mass of the added nano-object and not on the size of the resonator or the position of the nano-object attached to movable wall.

The possibility of the similar resonator based on the relative vibrations of graphene layers is also considered.

Acknowledgments

This study was supported the Russian Foundation for Basic Research (Grants 08-02-00685 and 08-02-90049-Bel).

References

1. Ekinci, K. L., Yang, Y. T., and Roukes, M. L. (2003) Ultimate limits to inertial mass sensing based upon nanoelectromechanical systems. *J. Appl. Phys.*, 95: 2682–2689.
2. Ilic, B., Craighead, H. G., Krylov, S., Senaratne, W., and Ober, C. (2004) Attogram detection using nanoelectromechanical oscillators. *J. Appl. Phys.*, 95: 3694–3703.
3. Peng, H. B., Chang, C. W., Aloni, S., Yuzvinsky, T. D., and Zettl, A. (2006) Ultrahigh frequency nanotube resonators. *Phys. Rev. Lett.*, 97: 087203-1-4.
4. Jensen, K., Kwanpyo, K., and Zettl, A. (2008) An atomic-resolution nanomechanical mass sensor. *Nature Nanotechnology*, 3: 533–537.
5. Kwon, Y. K. and Tomanek, D. (1998) Electronic and structural properties of multi-walled carbon nanotube. *Phys. Rev. B*, 58: 16001–16004.
6. Charlier, J.-C. and Michenaud, J. P. (1993) Energetics of multilayered carbon tubules. *Phys. Rev. Lett.*, 70: 1858–1861.
7. Belikov, A. V., Lozovik, Yu. E., Nikolaev, A. G., and Popov, A. M. (2004) Double-walled nanotubes: Classification and barriers to walls relative rotation, sliding and screwlike motion. *Chem. Phys. Lett.*, 385: 72–78.
8. Damnjanovic, M., Dobardzic, E., Milosevic, I., Vukovic, T., and Nikolic, B. (2003) Lattice dynamics and symmetry of double wall carbon nanotubes. *New J. Phys.*, 5: 148-1-15.
9. Bichoutskaia, E., Popov, A. M., El-Barbary, A., Heggie, M. I., and Lozovik, Yu. E. (2005) Ab initio study of relative motion of walls in carbon nanotubes. *Phys. Rev. B*, 71: 113403-1-9.
10. Bichoutskaia, E., Popov, A. M., Heggie, M. I., and Lozovik, Yu. E. (2006) Interwall interaction and elastic properties of carbon nanotubes. *Phys. Rev. B*, 73: 045435-1-9.
11. Ershova, O. V., Lozovik, Yu. E., Popov, A. M., Bubel', O. N., Kislyakov, E. F., Poklonskii, N. A., Knizhnik, A. A., and Lebedeva, I. V. (2008) Control of the motion of nanoelectromechanical systems based on carbon nanotubes by electric fields. *JETP*, 107: 653–661.
12. Lebedeva, I. V., Knizhnik, A. A., Popov, A. M., Lozovik, Yu. E., and Potapkin, B. V. (2009) Dissipation and fluctuations in nanoelectromechanical systems based on carbon nanotubes, *Nanotechnology*, 20: 105202-1-13.
13. http://amber.scripps.edu
14. Popov, A. M., Lozovik, Yu. E., Sobennikov, A. S., and Knizhnik, A. A. (2009) Nanomechanical properties and phase transitions in a double-walled (5,5)@(10,10) carbon nanotube: Ab initio calculations. *JETP*, 108: 621–628.
15. Barreiro, A., Rurali, R., Hernandez, E. R., Moser, J., Pichler, T., Forro L., and Bachtold, A. (2008) Subnanometer motion of cargoes driven by thermal gradients along carbon nanotubes. *Science*, 320: 775–778.
16. Grace, I. M., Bailey, S. W., and Lambert, C. J. (2004) Electron transport in carbon nanotube shuttles and telescopes. *Phys. Rev. B*, 70: 153405-1-4.
17. Bichoutskaia, E., Popov, A. M., Lozovik, Yu. E., Ivanchenko, G. S., and Lebedev, N. G. (2007) Electromechanical nanothermometer. *Phys. Lett. A*, 366: 480–486.
18. Brenner, D. W., Shenderova, O. A., Harrison, J. A., Stuart, S. J., Ni, B., and Sinnott, S. B. (2002) A second-generation reactive empirical bond order (REBO) potential energy expression for hydrocarbons. *J. Phys.: Condens. Matter*, 14: 783–802.